Regulation of murine normal and stress-induced erythropoiesis by Desert Hedgehog

*Ching-in Lau,[1] *Susan V. Outram,[1,2] José Ignacio Saldaña,[1] Anna L. Furmanski,[1] Johannes T. Dessens,[3] and Tessa Crompton[1]

[1]Immunobiology Unit, University College London Institute of Child Health, London, United Kingdom; [2]School of Health and Bioscience, University of East London, Stratford, United Kingdom; and [3]Department of Pathogen Molecular Biology, London School of Hygiene and Tropical Medicine, London, United Kingdom

The function of Hedgehog signaling in hematopoiesis is controversial, with different experimental systems giving opposing results. Here we examined the role of Desert Hedgehog (Dhh) in the regulation of murine erythropoiesis. Dhh is one of 3 mammalian Hedgehog family proteins. Dhh is essential for testis development and Schwann cell function. We show, by analysis of Dhh-deficient mice, that Dhh negatively regulates multiple stages of erythrocyte differentiation. In Dhh-deficient bone marrow, the common myeloid progenitor (CMP) population was increased, but differentiation from CMP to granulocyte/macrophage progenitor was decreased, and the mature granulocyte population was decreased, compared with wild-type (WT). In contrast, differentiation from CMP to megakaryocyte/erythrocyte progenitor was increased, and the megakaryocyte/erythrocyte progenitor population was increased. In addition, we found that erythroblast populations were Dhh-responsive in vitro and ex vivo and that Dhh negatively regulated erythroblast differentiation. In Dhh-deficient spleen and bone marrow, BFU-Es and erythroblast populations were increased compared with WT. During recovery of hematopoiesis after irradiation, and under conditions of stress-induced erythropoiesis, erythrocyte differentiation was accelerated in both spleen and bone marrow of Dhh-deficient mice compared with WT. (*Blood*. 2012;119(20):4741-4751)

Introduction

The Hedgehog (Hh) family of secreted intercellular signaling proteins are essential for the development of many tissues during embryogenesis and are also involved in the homeostasis of adult tissues, including skin, gut, bone, and thymus.[1-4] Their role in the regulation of hematopoiesis, however, has proved controversial, with different experimental models supporting opposing interpretations.[5-13] Here, we investigate erythropoiesis in Desert Hh (Dhh)–null adult mice and show that Dhh is a negative regulator of normal and stress-induced erythropoiesis.

There are 3 mammalian Hh proteins, with distinct patterns of expression and functions: Sonic Hh (Shh), Indian Hh (Ihh), and Dhh. Shh and Ihh are each essential for mouse development, whereas Dhh mutant mice are healthy and appear normal, although males are infertile.[14-16] Shh is most pleiotrophic of the family members and is essential for development of many tissues and organs, including brain, heart, lungs, limbs, and thymus.[16,17] Ihh has some overlapping functions with Shh and is essential for bone differentiation[15,18,19] and the regulation of thymocyte differentiation.[2] In contrast, the functions of Dhh seem to be more limited to testis development and Schwann cell function, hence the viability and lack of obvious phenotype of Dhh-deficient animals.[14,20]

The Hh proteins share a common signaling pathway, which is initiated when the Hh ligand binds to its cell-surface receptor Patched (Ptch). This releases Ptch's inhibition of the signaling molecule Smoothened (Smo), allowing transduction of the Hh signal into the cell, and activation of the Hh-responsive transcription factors, glioblastoma-associated protein 1 (Gli1), Gli2, and Gli3.[21,22] The Hh signaling pathway is regulated by multiple positive and negative feedback, and both *Ptch* and *Gli1* are themselves Hh target genes.[22,23] Gli1 is not essential for mouse development or Hh signaling; and as it is itself an Hh target gene, measurement of its transcription can be used as a read-out of Hh signaling in a given population of cells.[24]

Studies on the role of the Hh signaling pathway in hematopoiesis have led to conflicting results. In zebrafish, mutants of the Hh pathway have defects in hematopoietic stem cell (HSC) formation and definitive hematopoiesis.[25] In vitro studies also support the idea that Hh signaling is important for HSC proliferation and hematopoiesis.[26-28] Likewise, analysis of Ptch$^{+/-}$ mice, in which Hh signaling is increased, showed that Hh pathway activation caused cycling and expansion of BM hematopoietic cells, leading to HSC exhaustion.[29] In one report, conditional deletion of Smo, the nonredundant Hh pathway signal transduction molecule, suggested that HSCs require Hh signals for their homeostasis.[9] This was in contrast to 2 studies, which showed that conditional deletion of Smo had no impact on HSC function or hematopoiesis.[6,7]

Analysis of mutants in Shh, Ihh, Gli2, Gli3, and Smo have shown that Hh signaling is involved in T-cell development.[2,17,30-33] Analysis of Gli1-null mice has indicated that Gli1 also plays a role in HSC homeostasis, myeloid differentiation, stress-induced hematopoiesis, and thymocyte development.[5,34] Ihh has been shown to be involved in the induction of hematopoietic cell fate and terminal erythroid differentiation in the embryo.[10,13] In addition, in a recent report, Ptch mutation or conditional deletion of Smo has shown that Hh signaling is involved in BMP4-dependent stress-induced erythropoiesis in the mouse spleen.[35] Thus, the role of Hh signaling in the regulation of hematopoiesis and erythropoiesis is controversial and requires further investigation.[12]

Submitted October 20, 2011; accepted March 25, 2012. Prepublished online as *Blood* First Edition paper, March 28, 2012; DOI 10.1182/blood-2011-10-387266.

The publication costs of this article were defrayed in part by page charge payment. Therefore, and solely to indicate this fact, this article is hereby marked "advertisement" in accordance with 18 USC section 1734.

*C.-i.L. and S.V.O. contributed equally to this study.

The objective of this study was to examine the requirement for Dhh in erythropoiesis in the spleen and BM. Erythrocytes, like other blood lineages, develop from HSCs through a sequence of well-defined intermediates. In mice, HSC have been defined by their absence of lineage-specific markers, and expression of Sca-1 and c-kit, and are therefore referred to as $Lin^{-}Sca\text{-}1^{+}c\text{-}kit^{+}$ (LSK) stem cells. LSKs give rise to severalprogenitor cells, including common myeloid progenitor cells (CMP), which in turn give rise to granulocyte/macrophage progenitor cells (GMP) and megakaryocyte/erythroid progenitor cells (MEP). The MEP then give rise to the erythroid lineage, first by differentiating into burst-forming unit cells (BFU-E), the first erythroid committed cells, and then colony-forming units (CFU-E).[36] BFU-E and CFU-E cannot be identified by cell surface markers, so are quantified by their ability to produce colonies in functional assays in vitro. These cells then develop through a series of erythroblast stages, which are defined by surface expression of CD71 and Ter119.[37] $Ter119^{med}CD71^{hi}$ (population I, proerythroblast) precursors differentiate to $Ter119^{hi}CD71^{hi}$ (population II, basophilic erythroblast), which then down-regulate CD71 to become $Ter119^{hi}CD71^{med}$ (population III, polychromatophilic erythroblast) and then $Ter119^{hi}CD71^{-}$ (population IV, orthochromatic erythroblast) cells. At the later erythroblast stages, the nucleus progressively shrinks and is shed before the cells become mature erythrocytes.[38] The developmental program from HSCs to mature erythrocyte is regulated by complex transcriptional networks and by environmental signals.[39,40] In the adult, most erythropoiesis occurs in the BM, but under conditions of erythropoietic stress (anemia, hypoxia), the number of erythrocytes is increased, and this process of stress-induced erythropoiesis occurs predominantly in the spleen.[35,41]

Here, we show that Dhh functions as a negative regulator of normal and stress-induced erythropoiesis, at multiple stages of differentiation, in both the spleen and BM.

Methods

Mice

C57BL/6 mice (B&K Universal Ltd), $Dhh^{+/-}$ mice,[14] a gift from Andrew McMahon (Harvard University), backcrossed onto C57BL/6 mice for more than 8 generations, were bred and maintained at University College London. In some experiments, mice were irradiated with 4 Gy from a ^{60}Co γ-ray source, or anemia was induced by intraperitoneal injection of phenylhydrazine (60 mg/kg body weight; Sigma-Aldrich). All animal work was carried out under the United Kingdom Home Office regulations under the United Kingdom Home Office (Project License PPL 70/7088).

Flow cytometry, histology, staining, and antibodies

BM was isolated from femur. Cell suspensions from spleen and BM were prepared, stained and analyzed as described,[17,42] using directly conjugated antibodies from BD Biosciences PharMingen and eBioscience. Data are representative of more than 3 experiments. Statistical analysis was unpaired Student *t* test (equal or unequal variance depending on data). For some experiments, BM cells and splenocytes were isolated and sorted using MoFlo XDP Sorter (Beckman Coulter) to obtain populations of $Ter119^{+}$ and $CD71^{+}$ erythroblast populations, after magnetic bead depletion for cells positive for CD3, CD4, CD8, B220, Mac-1, and Gr-1. Staining with $CD71^{FITC}$ and $TER119^{PE}$ allowed sorting of early stage (I) to late stage (IV) erythroblast populations. Propidium iodide (PI) staining was carried out on magnetic-bead purified populations as described and examined using FACSCalibur (BD Biosciences).[33] For anti-Smo staining, cells were first incubated for 30 minutes in PBS with 1.5% donkey serum (Santa Cruz Biotechnology). After washing with PBS, cells were incubated with 0.5 μg anti-CD16/CD32 in 50 μL of PBS for 5 minutes, then incubated with 2 μg anti-Smo N-19 (Santa Cruz Biotechnology) or goat IgG (Santa Cruz Biotechnology), as isotype control, in 50 μL of PBS for 60 minutes and washed with PBS and 0.5% BSA. Cells were then incubated with 2 μg of biotin-conjugated $F(ab')_2$ fragment of donkey anti–goat IgG in 50 μL of PBS and 1.5% donkey serum for 30 minutes and washed with PBS and 0.5% BSA. Cells were finally incubated with: $streptavidin^{cychrome}$, anti-$CD71^{FITC}$, anti-$TER119.^{PE}$ For anti-Ptch staining, cells were first incubated for 30 minutes in PBS with 1.5% rat serum (Santa Cruz Biotechnology). After washing with PBS, cells were incubated with 0.5 μg anti-CD16/CD32 in 50 μL of PBS for 5 minutes, then incubated with 2 μg anti-Ptch (R&D systems) or rat IgG (Santa Cruz Biotechnology), as isotype control, in 50 μL of PBS for 60 minutes and washed with PBS and 0.5% BSA. Cells were then incubated with 2 μg of biotin-conjugated anti–rat IgG in 50 μL of PBS and 1.5% rat serum for 30 minutes and washed with PBS and 0.5% BSA. Cells were finally incubated with: $streptavidin^{PE}$, anti-$CD71^{FITC}$, and anti-$TER119^{PerCP.Cy5.5.}$

For assessment of reticulocytes in blood, reticulocytes were counted from Giemsa-stained blood films.

For histology, spleens were fixed in phosphate-buffered formalin (10% volume/volume), paraffin-embedded, and sectioned for H&E staining, by standard protocols. Pictures were photographed by Leica DFC320 digital camera (Leica Microsystems) with Leica DMIL Microscope (Leica Microsystems), and acquired by software Leica Qwin vLite3.2.1 (Leica Microsystems).

Quantification of red pulp (RP) and white pulp (WP) surface area on H&E-stained sections was carried out using ImageJ v1.45b software http://imagej.nih.gov/ij/).

Hematopoietic colony assay

Colony-forming assays were performed using methocult methylcellulose-based medium (StemCell Technologies). A total of 2×10^6 BM cells and 2×10^7 spleen cells were plated in 1 mL of methylcellulose medium (M3334 and M3434) in a 35-mm culture dish (StemCell Technologies). Cultures were incubated at 37°C in 5% CO_2. BFU-E on methylcellulose medium M3434 was counted after 7 days.

Cell culture and purification

BM cells and splenocytes were isolated and cultured at a concentration of 5×10^6 cells/mL in AIM-V medium at 37°C and 5% CO_2. Cells were harvested at 18 hours and $Ter119^{+}$ erythroblast populations purified by magnetic bead separation using the EasySep Biotin positive selection kit (StemCell Technologies) according to the manufacturer's instructions.

Genotyping and PCR analysis

Animals were genotyped by PCR. DNA extraction and PCR analysis were as described,[17] using approximately 0.5 μg genomic DNA as template. Primers are as follows: For mutated *Dhh* allele, *Dhh/neo* forward, GGCATGCTGGGGATGCGGTG; reverse, CCAGGAAGACGAGCACTGGCGTG; and wild-type (WT), *Dhh* forward, ATCCACGTATCGGTCAAAGC; and reverse, GGTCCAGGAAGAGCAGCAC.

Quantitative RT-PCR

RNA extraction and cDNA synthesis were as described.[33] One primer for each pair was designed to span exon-exon boundaries to avoid amplification of genomic DNA. The following primers were used: *Gapdh* forward, CCTGGAGAAACCTGCCAAGTATG; reverse, AGAGTGGGAGTTGCTGTTGAAGTC; *Smo* forward, TTCTTCAACCAGGCTGAGTG; reverse, CGTATGGCTTCTCATTGGAGTG; and *Ptch* forward, TGCTCTCCAGTTCTCAGACTC; reverse, CCACAACCTTGGGTTTGG. *HPRT* and *Gli1* primers were as described.[43]

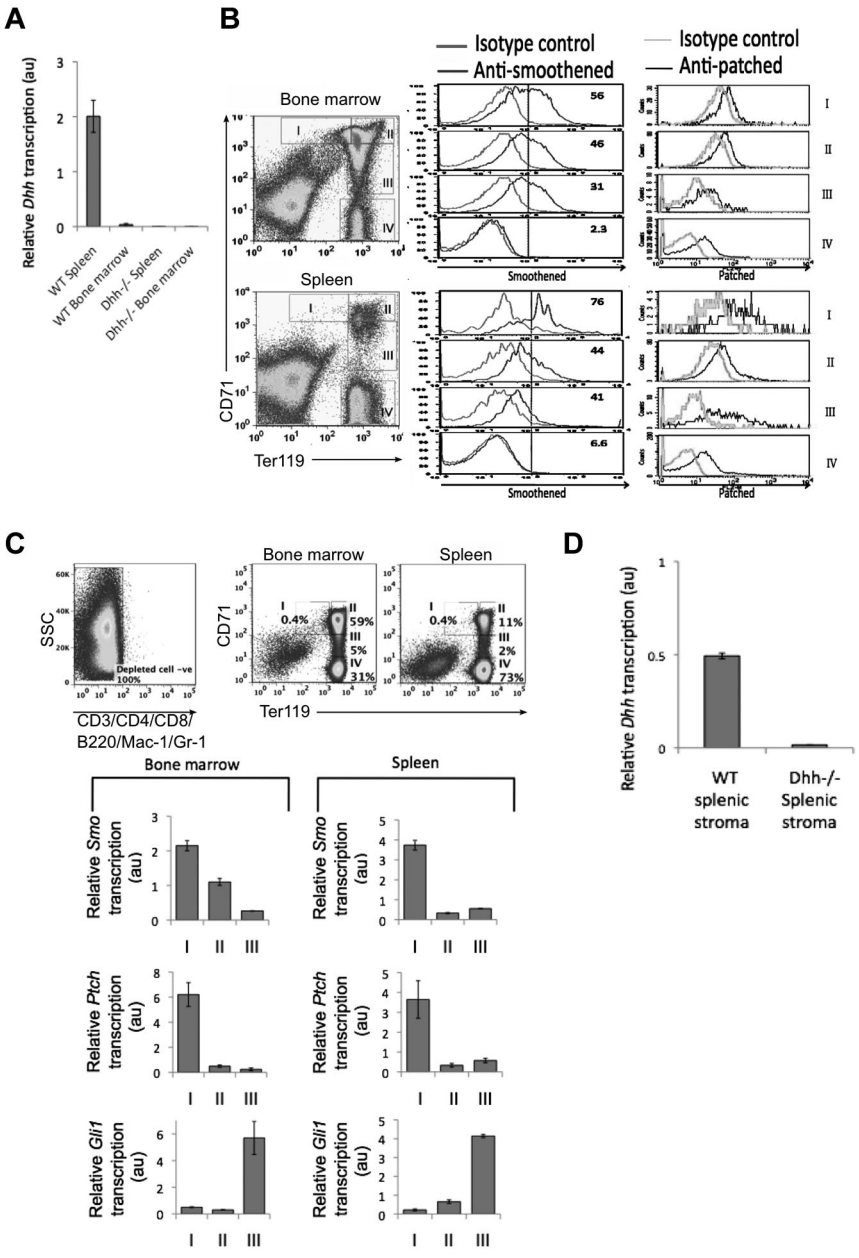

Figure 1. Components of the Hh pathway are expressed in erythroblasts in spleen and BM. (A) Quantitative RT-PCR of *Dhh* expression in WT and Dhh$^{-/-}$ spleen and bone marrow. (B) Histograms represent anti-Smo staining (left column) and anti-Ptch staining (right column), gated on erythroblast populations I to IV, as defined by Ter119 and CD71 expression (dot plots). Top panel represents WT BM; and bottom panel, WT spleen. (C) Quantitative RT-PCR analysis in sorted erythroblast populations I to III from WT BM. Dot plots represent sorting strategy. Cells were first magnetic bead–depleted to remove lymphocyte, macrophage, and granulocyte populations, and the negative populations (negative for CD3, CD4, CD8, B220, Mac-1, and Gr-1, left dot plot) were then stained with anti-CD71 and anti-Ter1119. Gates used for sorting are shown for BM (middle dot plot) and spleen (right dot plot). Bar charts represent *Smo*, *Ptch*, and *Gli1* expression in BM (left) and spleen (right). (D) Quantitative RT-PCR of *Dhh* expression in WT and Dhh$^{-/-}$ splenic stroma.

Results

Dhh and components of the Hh signaling pathway are expressed in adult spleen and bone marrow

Given that the involvement of Hh proteins in erythropoiesis is controversial, we investigated the possible function of Dhh in erythropoiesis. We therefore first considered whether Dhh is expressed in the adult spleen and BM, comparing expression between WT and Dhh$^{-/-}$, as negative control. We found *Dhh* transcription, by quantitative RT-PCR, in WT spleen, but not Dhh$^{-/-}$ spleen, and we were also able to detect *Dhh* transcription in WT BM (Figure 1A). This is consistent with recent reports that Dhh is expressed in stromal cells in the BM, and by nonhematopoetic cells of the spleen stroma.[35,44]

As Dhh is expressed in tissues where erythropoiesis occurs, we tested whether developing erythrocyte-lineage cells express components of the Hh signaling pathway. We stained the 4 erythrocyte-committed erythroblast populations, defined by Ter119 and CD71 expression, with antibodies directed against the Hh-signal transduction molecule Smo and the cell surface Hh-receptor Ptch (Figure 1B). In cells isolated from both spleen and BM, we found highest Smo expression on the most immature erythroblast population I (Ter119^{med}CD71^{hi}), with gradual reduction in cell surface expression in each subsequent population, so that population IV did not express detectable cell-surface Smo. In contrast, cell surface expression of Ptch was detectable on all erythroblast populations, consistent with its potential function as an Hh-sequestering protein.

To assess expression of the Hh target genes/signaling genes in erythroblast populations, we sorted populations I to III from BM

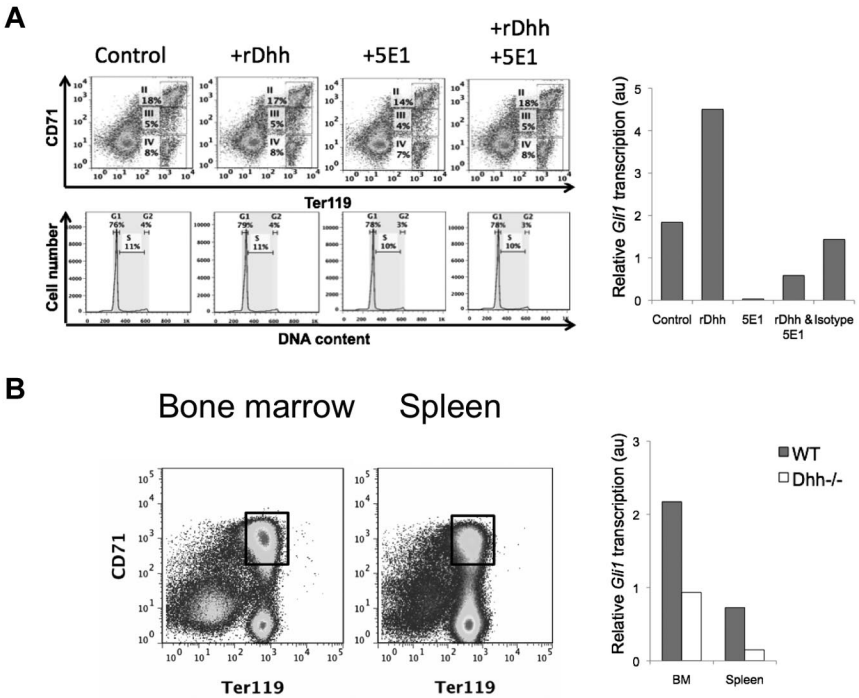

Figure 2. Erythroblasts are Hh responsive in vitro and in vivo. (A) BM was cultured for 18 hours, control or treated with rDhh, anti-Hh mAb (5E1), rDhh and 5E1 together, and isotype control mAb. After culture, cells were stained with anti-CD71 and anti-Ter119 to confirm that the short treatment had not changed the relative distribution of the subsets (top panel dot plots), and with PI to confirm that survival/cell cycle status was not affected (middle panel, histograms) in erythroblasts. Erythroblasts II to IV were purified from each culture by magnetic bead purification for Ter119$^+$ cells, and RNA prepared for quantitative RT-PCR analysis of *Gli1* expression (bar chart). (B) Erythroblast population II was sorted from magnetic bead lymphocyte-depleted cells from BM (left dot plot) and spleen (right dot plot). Gates used for sorting are shown. Bar chart represents *Gli1* expression, measured by quantitative RT-PCR, on RNA prepared from population II sorted from WT (filled bars) and Dhh$^{-/-}$ (open bars) BM and spleen.

and spleen and performed quantitative RT-PCR for analysis of transcription of *Ptch*, *Smo*, and *Gli1* (Figure 1C). We did not carry out this analysis on population IV because the RNA isolated from these cells was of poor quality, as the nucleus is shrinking and will be shed. Transcription of *Smo* was highest in population I, and down-regulated in populations II and III, in cells sorted from both BM and spleen. Transcription of *Ptch*, the cell surface receptor for Hh proteins, mirrored that of *Smo*, with highest expression in population I, and reduced but detectable expression in populations II and III. Interestingly, we found highest expression of the Hh-responsive target gene *Gli1* in the later population III. The fact that *Smo* and *Ptch* transcription are highest in population I suggests that these cells transduce the strongest Hh signal. Gli1 is not required to initiate the Hh signal but is up-regulated in response to it, consistent with the fact that the highest level *Gli1* expression was observed in the later population III. This pattern of expression is similar to that observed during thymocyte development, where the earliest progenitors express highest levels of Smo, but *Gli1* expression peaks at a later stage.[2,31]

We did not detect *Dhh* expression in erythroblast populations I to III from either spleen or BM (data not shown), and a previous study has located Dhh protein expression to spleen stroma by immunohistochemistry.[35] To confirm this, we prepared RNA from splenic rudiment (stroma) and carried out quantitative RT-PCR. Transcription of *Dhh* was detected in WT spleen stroma, but not stroma from Dhh$^{-/-}$ spleen (Figure 1D).

Erythroblasts are Dhh-responsive in vitro and ex vivo

To verify that erythroblasts are capable of transducing a Dhh signal, we treated WT BM for 18 hours with recombinant (r) Dhh, neutralizing anti-Hh mAb 5E1, both treatments together, or isotype control mAb, and purified Ter119$^+$ cells from the cultures by magnetic bead separation, for RNA preparation. To test whether the treatments caused changes in the cellular composition of the Ter119$^+$ population (subsets II-IV) during the short culture period, we analyzed the cultures for CD71 and Ter119 expression, and cell cycle/survival status. Viability was good, and we found no difference between the conditions in relative composition of the erythroblast subsets, cell cycle, or survival status after culture (Figure 2A), confirming that it was reasonable to carry out the *Gli1* expression studies on the Ter119$^+$ population. Treatment with rDhh increased expression of the Hh-target gene *Gli1*, whereas neutralization of Hh by 5E1 treatment down-regulated *Gli1* transcription. The addition of rDhh to 5E1 treatment partially recovered *Gli1* transcription, confirming specificity of the reagents, whereas treatment with an isotype-control antibody did not significantly affect *Gli1* transcription (Figure 2A).

To assess the impact of Dhh on Hh signal transduction in erythroblasts ex vivo, we sorted erythroblast population II from WT and Dhh$^{-/-}$ BM and spleen and again measured transcription of the Hh-target gene *Gli1* (Figure 2B). Expression of *Gli1* was approximately 6-fold higher in WT erythroblasts compared with their Dhh$^{-/-}$ counterparts in spleen, and approximately 2.25-fold higher in WT erythroblasts compared with Dhh$^{-/-}$ in BM, indicating that Dhh signal transduction is active in developing WT erythroblasts and accounts for most Hh-dependent transcription in these cells. The fact that some *Gli1* expression was detectable in the Dhh$^{-/-}$ cells indicated that erythroblasts were also transducing signals from either Ihh or Shh in both BM and spleen, hence the remaining *Gli1* expression.

Taken together, these experiments show that developing erythroblasts undergo active Dhh signaling during their differentiation in the spleen and BM.

Abnormal erythropoiesis in Dhh$^{-/-}$ mice

Given that Dhh is expressed at sites of erythropoiesis and differentiating cells of the erythroid lineage transduce Hh signals, we asked if Dhh plays a role in the regulation of erythropoiesis, by analysis of Dhh$^{-/-}$ mice. We found that the spleen of Dhh$^{-/-}$ mice

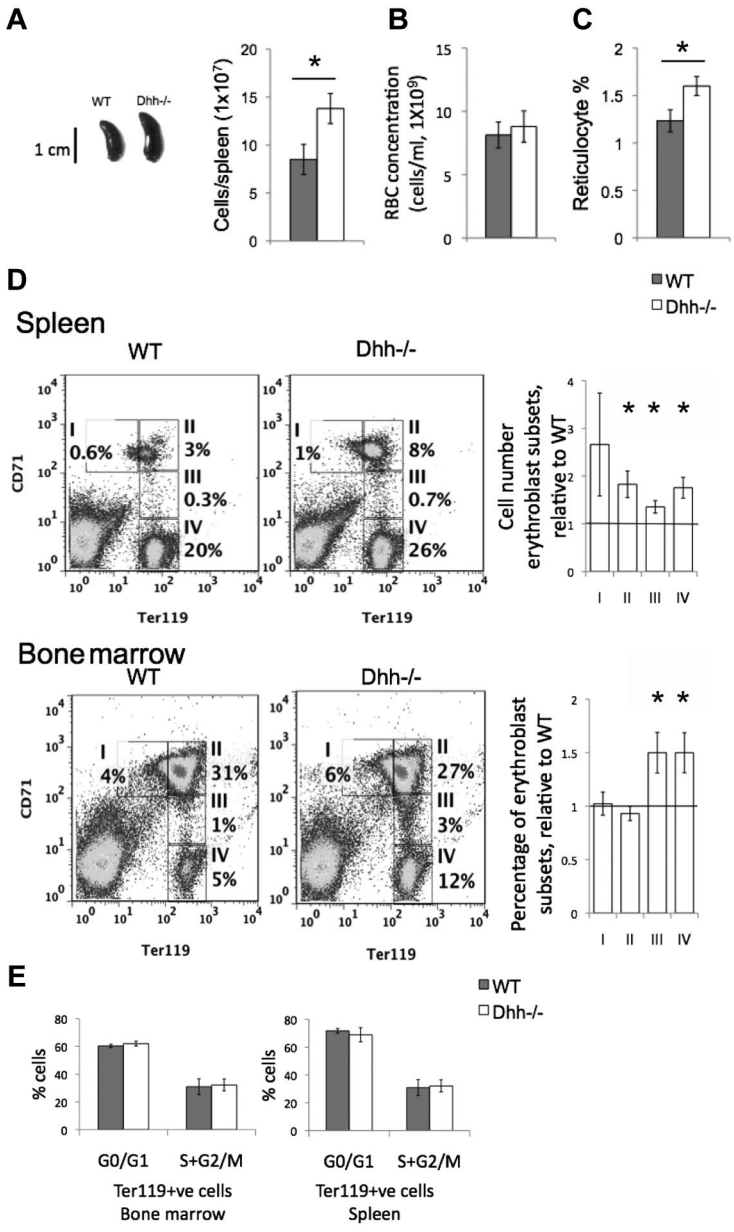

Figure 3. Abnormal erythropoiesis in Dhh$^{-/-}$ mice. (A) Photograph represents typical spleen from WT (left) and Dhh$^{-/-}$ (right). Histogram represents the mean spleen cell number from WT and Dhh$^{-/-}$. The difference in mean between WT and Dhh$^{-/-}$ is statistically significant ($P = .003$). (B) Bar chart represents the mean RBC count in WT (8.1×10^9/mL, shaded bar) and Dhh$^{-/-}$ (8.8×10^9/mL, open bar) blood. (C) Bar chart represents the mean percentage of reticulocytes in RBCs from WT (shaded bar) and Dhh$^{-/-}$ (open bar) blood. The increase in mean percentage of reticulocytes in Dhh$^{-/-}$ compared with WT was statistically significant ($P = .014$). (D) Spleen (top panel) and BM (bottom panel) cells from WT and Dhh$^{-/-}$ were stained with antibodies against CD71 and Ter119. Dot plots represent the percentage of cells in the 4 erythroblast subsets (I-IV), defined by CD71 and Ter119 expression, as shown in the regions indicated, in WT (left) and Dhh$^{-/-}$ (right). For spleen, bar charts represent the mean of the number of cells in each erythroblast subset in Dhh$^{-/-}$, divided by the number of cells in their counterpart subset in WT spleen, for each erythroblast population. The difference between the mean of Dhh$^{-/-}$ and WT was statistically significant for population II ($P = .012$), population III ($P = .015$), and population IV ($P = .006$). For BM, the bar chart represents the mean relative percentage of erythroblast populations I to IV, in Dhh$^{-/-}$, relative to WT littermate. The difference between the means of Dhh$^{-/-}$ and WT was statistically significant for population III ($P = .022$) and population IV ($P = .02$). (E) Cell cycle analysis of erythroblasts from WT and Dhh$^{-/-}$ BM and spleen. Bar charts represent the mean percentage of cells in G_0/G_1 and $S + G_2/M$, as assessed by PI staining and flow cytometry in magnetic-bead-purified Ter119$^+$ cells from WT (filled bars) and Dhh$^{-/-}$ (open bars) BM (left) and spleen (right). There were no significant differences between WT and Dhh$^{-/-}$ in either BM or spleen.

was larger than that of WT littermates (Figure 3A). There was no significant difference in total red blood cell (RBC) counts in Dhh$^{-/-}$ blood compared with WT, but the number of reticulocytes in the blood was significantly increased (Figure 3B-C). In the spleen, there was an increase in each population of erythroblasts (populations I to IV; Figure 3D). In the BM, we found a statistically significant increase in the proportions of erythroblast populations III and IV (Figure 3D). The increase in reticulocytes in the Dhh$^{-/-}$ blood and in erythroblast populations in the Dhh$^{-/-}$ BM and spleen indicated that Dhh is a negative regulator of erythropoiesis. There are several possible mechanisms that might contribute to, or account for, the increased erythropoiesis in Dhh$^{-/-}$ mice. First, the absence of Dhh might increase the proliferation of the erythroblast subsets. Second, it might influence the frequency of the precursors that give rise to them. Third, the absence of Dhh might increase the rate of erythroblast differentiation between the different stages to produce more reticulocytes.

To distinguish between these possibilities, we first assessed the cell-cycle status of the erythroblast populations by PI staining of Ter119$^+$ cells isolated from Dhh$^{-/-}$ and WT spleen and BM. There was no significant difference in the proportion of cells in $S + G_2/M$ between Dhh$^{-/-}$ and WT in either spleen or BM (Figure 3E). These experiments indicated that Dhh does not act as a negative regulator of proliferation of erythroblast cells but more likely regulates an earlier precursor and/or the rate of differentiation along the erythrocyte lineage.

We therefore tested the ability of progenitors from Dhh$^{-/-}$ and WT spleen and BM to differentiate along the erythroid lineage in vitro, by assessment of their ability to form BFU. We found a statistically significant increase in BFU-Es in both BM and spleen from Dhh$^{-/-}$ compared with WT (Figure 4A).

These data show that Dhh is a negative regulator of erythropoiesis, so we examined its influence on earlier hematopoietic populations. We found no difference in the relative proportions of

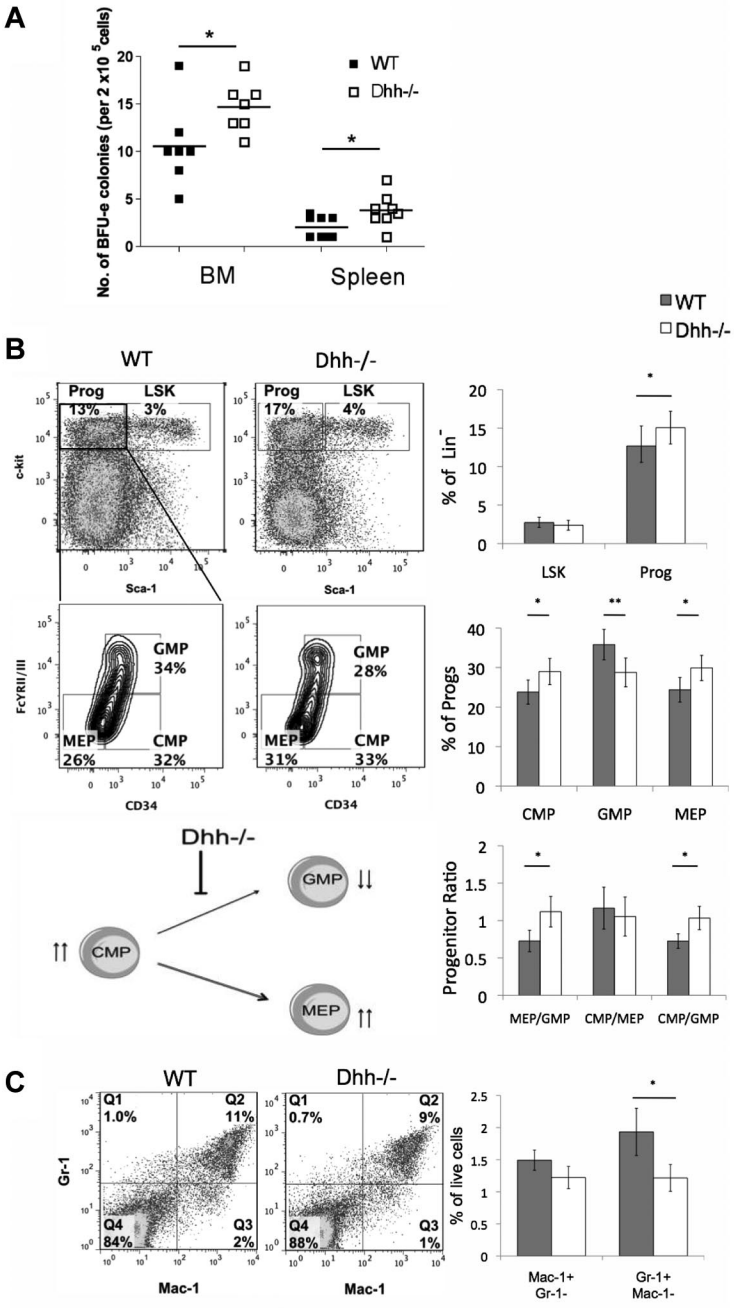

Figure 4. Dhh influences early erythropoiesis and progenitor differentiation. (A) Scatter plot represents BFU assays, carried out on BM and spleen, from WT (filled squares) and Dhh$^{-/-}$ (open squares). The mean for each group is indicated with a line. The increase in mean number of colonies in Dhh$^{-/-}$ compared with WT is statistically significant for both BM ($P = .050$) and spleen ($P = .032$). (B) Dot plots represent analysis of LSK stem cells and Sca-1^{-}c-kit^{+} progenitors in WT (left) and Dhh$^{-/-}$ (right) BM, staining with antibodies against Sca-1 and c-kit, after exclusion of Lin^{+} cells. The bold region represents the gating used to analyze the Sca-1^{-} c-kit^{+} progenitor population. Contour plots represent the subdivision of the progenitor population from WT (left) and Dhh$^{-/-}$ (right), staining against CD34 and FcγRII/III, into CMP, GMP, and MEP. The percentage of progenitors in each subset and the regions used for their definition are shown. Top bar chart represents the mean percentage of Lin^{-} cells that are LSK (Sca-1^{+} c-kit^{+}) and progenitor (Sca-1^{-}c-kit^{+}) in WT (filled bars) and Dhh$^{-/-}$ (open bars) BM. The increase in the mean percentage of progenitors in the Dhh$^{-/-}$ compared with WT is statistically significant ($P = .019$). Middle bar chart represents the percentage of the progenitor population that is CMP, GMP, or MEP, as defined by CD34 and FcγRII/III expression, in WT (filled bars) and Dhh$^{-/-}$ (open bars). The difference in mean proportion is statistically significant between WT and Dhh$^{-/-}$ for CMP ($P = .05$), GMP ($P = .0006$), and MEP ($P = .005$). Bottom bar chart represents the mean progenitor ratio in WT (filled bars) and Dhh$^{-/-}$ (open bars). The difference in mean ratios between WT and Dhh$^{-/-}$ is statistically significant for MEP/GMP ($P = .009$) and CMP/GMP ($P = .024$), but not for CMP/MEP. The cartoon represents a summary of the effects of Dhh deficiency at this stage of differentiation. Absence of Dhh, reduced differentiation from CMP to GMP, and the GMP population are reduced. The CMP population is increased, and differentiation to MEP is favored. (C) Dot plot represents staining against Gr-1 and Mac-1 on BM cells from WT (left) and Dhh$^{-/-}$ (right). The percentage of cells in each quadrant is shown. Bar chart represents the mean percentage of BM cells that are macrophages (Mac-1^{+}Gr-1^{-}) and granulocytes (Mac-1^{-}Gr-1^{+}) in WT (filled bars) and Dhh$^{-/-}$ (open bars). The reduction in the mean percentage of granulocytes in Dhh$^{-/-}$ compared with WT is statistically significant ($P = .04$).

LSK stem cells, but the population of Sca-1^{-}c-kit^{+} progenitors was increased in Dhh$^{-/-}$ BM compared with WT (Figure 4B). When we gated on the progenitor population and subdivided it by expression of CD34 and FcγRII/III, we found that the proportion of the earlier CMP was increased in Dhh$^{-/-}$ compared with WT. There was also a statistically significant increase in the proportion of MEPs in the Dhh$^{-/-}$ compared with WT and a concomitant decrease in the proportion of GMP. Thus, the ratio of MEP to GMP was statistically increased in the Dhh$^{-/-}$ BM compared with WT (Figure 4B). When we compared the ratio of the precursor CMP population with each of its progeny populations, we found that, although the ratio of CMP/MEP was not different between Dhh$^{-/-}$ and WT, the ratio of CMP/GMP was statistically significantly increased. These data therefore indicate that Dhh acts on the CMP population: in the absence of Dhh, differentiation from CMP to GMP is decreased, whereas differentiation to the erythrocyte lineage (from CMP to MEP) continues at its normal rate; but given the increase in the progenitor CMP population, this results in an overall increase in differentiation to the erythroid lineage (Figure 4B). The proportion of granulocytes was significantly reduced in the Dhh$^{-/-}$ BM compared with WT (Figure 4C). Thus, Dhh negatively regulates early erythroid differentiation but is required for normal granulocyte production.

Dhh is a negative regulator of erythrocyte differentiation during recovery after irradiation

To test whether Dhh reduces the rate of differentiation along the erythrocyte lineage, we examined erythropoiesis under conditions

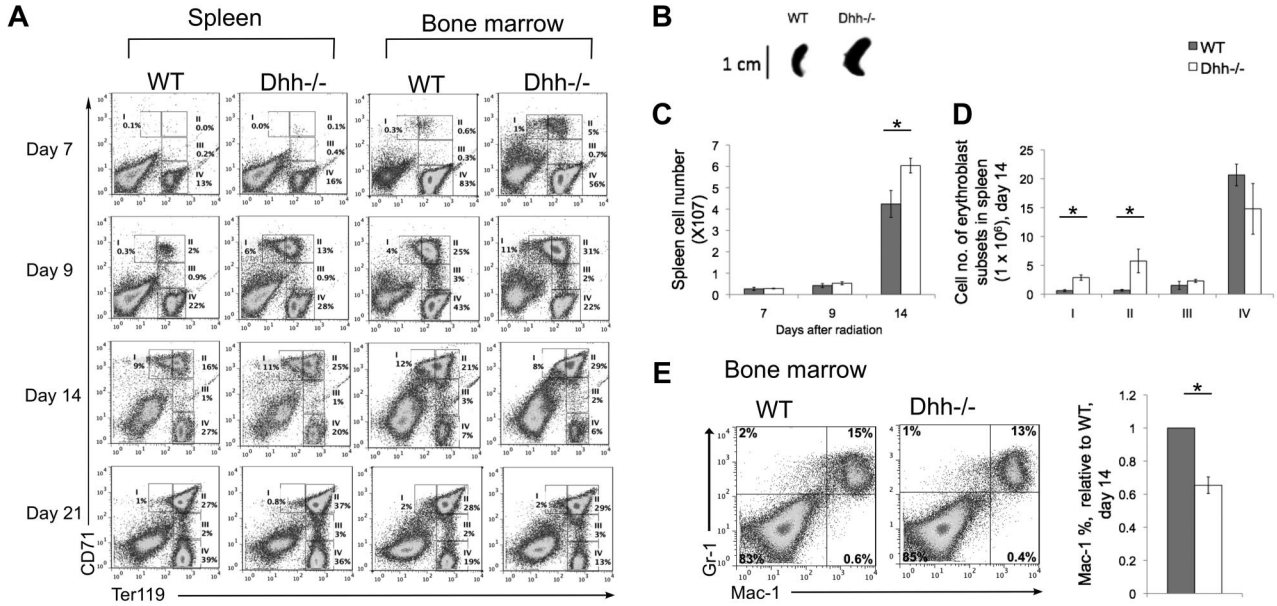

Figure 5. Acceleration of differentiation and recovery after irradiation in Dhh$^{-/-}$ mice. (A) Kinetics of recovery of the erythroblast populations after nonlethal irradiation was measured in the spleen (left panel) and BM (right panel) at 7 days (top row), 9 days (second row), 14 days (third row), and 21 days (fourth row) after irradiation. Dot plots represent erythroblast populations I to IV, defined by CD71 and Ter119 expression, and the regions used and percentage of cells in each population are shown. (B) Photograph represents typical spleen from WT (left) and Dhh$^{-/-}$ (right) at 14 days after irradiation. (C) Bar chart represents the mean spleen cell number after irradiation in WT (filled bars) and Dhh$^{-/-}$ (open bars). The increase in mean cell number in Dhh$^{-/-}$ compared with WT on day 14 is statistically significant ($P = .046$). (D) Bar chart represents the mean number of cells in each erythroblast subset in WT (filled bars) and Dhh$^{-/-}$ (open bars) in the spleen on day 14. The difference in mean between WT and Dhh$^{-/-}$ was statistically significant for population I ($P = .003$) and population II ($P = .044$). (E) Dot plot represents staining against Mac-1 and Gr-1 on day 14 after irradiation from WT (left plot) and Dhh$^{-/-}$ (right plot) BM. Bar chart represents the mean relative percentage of Mac1^{+} cells in WT (filled bars) and Dhh$^{-/-}$ (open bars) BM, 14 days after irradiation. The difference in mean relative percentage is statistically significant ($P < .001$).

in which hematopoiesis and erythropoiesis take place in a more or less synchronized wave, after recovery from sublethal irradiation. We depleted the hematopoetic system in Dhh$^{-/-}$ and WT littermates by sublethal irradiation. We then followed the regeneration of erythroblast populations in the spleen and BM for 3 weeks after irradiation. Erythropoiesis occurred more rapidly in both spleen and BM in Dhh$^{-/-}$ compared with WT, and both returned to pre-irradiation values by day 21 (Figure 5A). Population II was already present on day 7 on Dhh$^{-/-}$ spleen and BM, but not in WT. On day 14 after irradiation, the Dhh$^{-/-}$ spleen was significantly larger and contained more cells in subsets I and II than WT (Figure 5A-D). Staining with antibodies against Gr-1 and Mac-1 showed that the proportion of cells that were committed to the macrophage lineage (Mac-1^{+}) was significantly reduced in the Dhh$^{-/-}$ BM compared with WT (Figure 5E). Thus, as hematopoiesis recovers after irradiation, differentiation along the erythroid lineage was accelerated in the Dhh$^{-/-}$ BM and spleen compared with WT, whereas macrophage differentiation in the BM was reduced.

Dhh is a negative regulator of stress-induced erythropoiesis in the spleen

Under conditions of erythropoietic stress, the production of erythrocytes is increased, and the major site of erythropoiesis moves to the spleen.[41] To investigate the function of Dhh specifically in stress-induced erythropoiesis in the spleen, we treated Dhh$^{-/-}$ and WT mice with phenylhydrazine (PHZ) to cause anemia, and followed the kinetics of recovery of RBC counts and reticulocytes in the blood (Figure 6A) and erythroblast populations in the spleen and BM (Figure 6B). The Dhh$^{-/-}$ mice recovered more quickly than WT, and RBC counts had returned to normal in both by day 14 (Figure 6). Five days after treatment, the Dhh$^{-/-}$ spleen was larger than WT (Figure 6A). Erythropoiesis was strongly induced in both Dhh$^{-/-}$ and WT spleen, with an increase in erythroblast population II from less than 10% in untreated animals (Figure 3) to more than 50% at day 5 after PHZ treatment (Figure 6B). Interestingly, we also observed an increase in erythropoiesis in the BM after PHZ treatment in the Dhh$^{-/-}$ mice. At day 5 after treatment, the proportion of erythroblast population II was increased to 47% in the Dhh$^{-/-}$ BM, from approximately 27% in untreated Dhh$^{-/-}$ controls (Figures 3D and 6B). Seven days after treatment, the RBC count and reticulocyte count were significantly higher in the Dhh$^{-/-}$ blood compared with WT, although the proportion of reticulocytes was equivalent. Nine days after treatment, the Dhh$^{-/-}$ spleen was smaller than WT, and the proportion of blood reticulocytes was significantly lower (Figure 6B), consistent with accelerated differentiation in the Dhh$^{-/-}$, so that by day 9 its proportion of reticulocytes was already in decline, whereas in the WT it was still rising.

To determine whether Dhh deficiency influenced earlier stages of erythropoiesis after induction of anemia, we assessed the proportion of MEP cells (defined as Sca-1^{-}c-kit^{+} progenitors, which are CD34^{-} and FcγRII/III^{-}) in BM and spleen 7 days after PHZ treatment. In the BM, the proportion of MEP was significantly reduced in the Dhh$^{-/-}$ relative to WT (Figure 6C). Interestingly, the proportion of MEP was significantly increased in the Dhh$^{-/-}$ spleen, compared with WT spleen, consistent with increased mobilization of progenitors to the Dhh$^{-/-}$ spleen and the increase in erythropoiesis observed in the Dhh$^{-/-}$ spleen compared with WT. The proportion of Ly6g^{+}

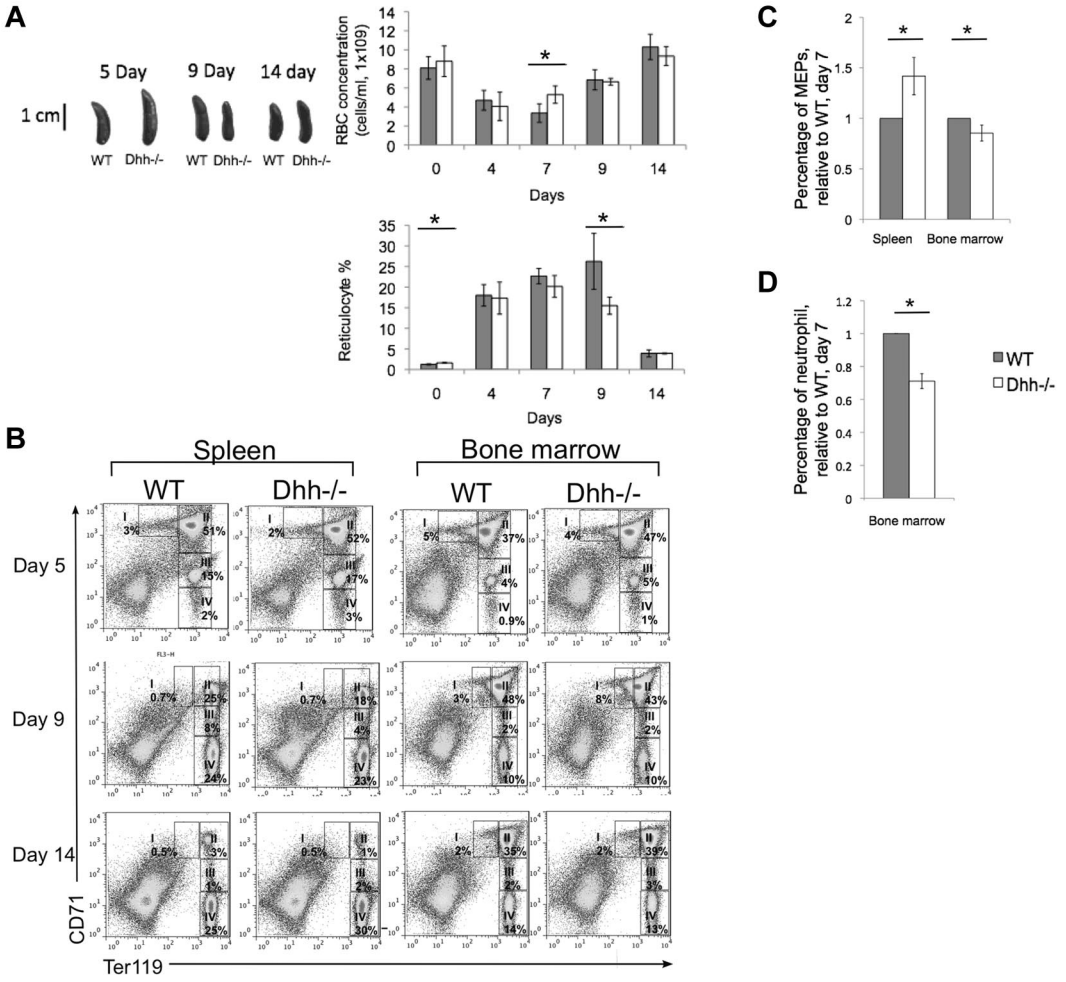

Figure 6. Dhh$^{-/-}$ mice recover more quickly during stress-induced anemia that WT. Anemia was induced in Dhh$^{-/-}$ and WT mice by PHZ treatment, and the kinetics of stress-induced erythropoiesis and recovery was monitored over time. (A) Photographs represent typical WT and Dhh spleen size at 5, 9, and 14 days after PHZ treatment. Top bar chart represents time course of RBC concentration in WT (filled bars) and Dhh$^{-/-}$ (open bars) blood, after PHZ treatment. The difference in mean RBC concentration between WT and Dhh$^{-/-}$ was statistically significant on day 7 ($P = .011$). Bottom bar chart represents the percentage of reticulocytes in RBCs in blood. The difference in mean percentage between WT and Dhh$^{-/-}$ was statistically significant before treatment (day 0, $P = .015$) and on day 9 ($P = .045$). (B) Kinetics of recovery of the erythroblast populations after PHZ treatment was measured in the spleen (left panel) and BM (right panel) at 5 days (top row), 9 days (second row), and 14 days (third row) after treatment. Dot plots represent erythroblast populations I to IV, defined by CD71 and Ter119 expression, and regions used and percentage of cells in each population are shown. (C) The relative percentage of MEP (measured by FACS, staining Lin$^-$ cells with antibodies against CD34 and FcγRII/III) in spleen (left) and BM (right) in WT (filled bars) and Dhh$^{-/-}$ (open bars), 7 days after PHZ treatment. The difference in mean was statistically significant for spleen ($P = .017$) and BM ($P = .033$). (D) The relative percentage of neutrophils (measured by FACS, staining with antibodies against Ly6g) in BM in WT (filled bars) and Dhh$^{-/-}$ (open bars), 7 days after PHZ treatment. The difference in means was statistically significant ($P < .001$).

cells (neutrophils) was significantly reduced in the Dhh$^{-/-}$ BM compared with WT (Figure 6D).

Dhh$^{-/-}$ spleen contains more RP areas than WT, and histology returns to normal more quickly on recovery from stress-induced erythropoiesis

Given that erythropoiesis was increased in Dhh$^{-/-}$ spleen compared with WT, both in normal conditions and after induction of anemia, we tested whether Dhh$^{-/-}$ spleen showed abnormal histology or a difference in the proportion of RP area, compared with WT. Hematoxilin and eosin staining on paraffin-embedded longitudinal spleen sections revealed normal histology, and RP and WP areas in both WT and Dhh$^{-/-}$ spleen (Figure 7A-B). We measured RP and WP surface area across the entire surface area of the central longitudinal spleen section and calculated the RP/WP ratio and the percentage of RP (Table 1). Consistent with the increased erythropoiesis in Dhh$^{-/-}$ spleen, the ratio of RP/WP was increased from 1.4 in WT to 2.1 in Dhh$^{-/-}$ spleen, and the percentage of RP increased from 59% in WT to 68% in Dhh$^{-/-}$ spleen. We then compared the induction of RP during stress-induced erythropoiesis caused by anemia after PHZ treatment (Figure 7C-J). In both WT and Dhh$^{-/-}$, the RP area was increased at 5 days after treatment to 84% and 83%, respectively (Figure 7C-D; Table 1). The RP area remained high at days 7 and 9 after treatment but resolved more quickly in the Dhh$^{-/-}$ than in the WT (Figure 7I-J), consistent with the faster resolution of the proportion of reticulocytes in the blood in the Dhh$^{-/-}$ (Figure 6A). Thus, on day 14 after treatment, the RP/WP ratio was reduced to 2.5 in Dhh$^{-/-}$ spleen and 3.7 in WT spleen.

The dynamics of RP induction and resolution therefore mirror the kinetics of erythrocyte differentiation in Dhh$^{-/-}$ and WT spleen, both under normal conditions (Figure 7A-B) and during stress-induced anemia (Figure 7C-J).

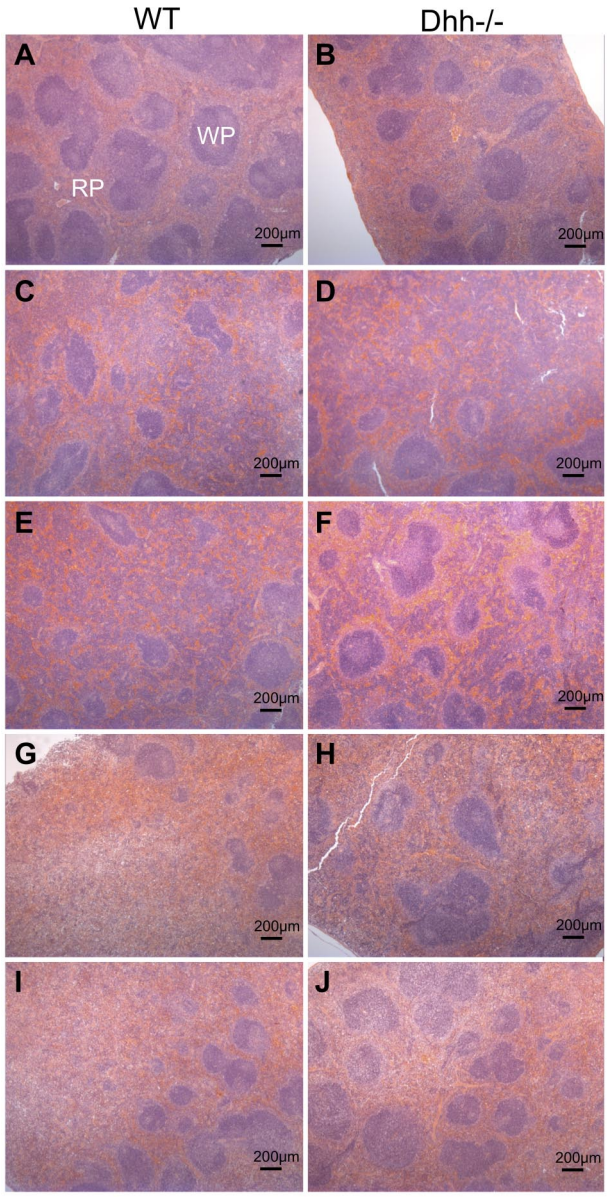

Figure 7. Histology showing red and WP areas in Dhh$^{-/-}$ and WT spleens, before and after induction of stress-induced erythropoiesis. Parafin-embedded spleen sections were stained with hematoxilin and eosin, to identify WP areas, which stained deeper purple, and RP areas, which stained pink. Typical WP and RP are illustrated in panel A. Left column (A,C,E,G,I) represents typical histology in WT spleens; and right column (B,D,F,H,J), typical histology in Dhh$^{-/-}$ spleen, without treatment (A-B) and during a time course after induction of stress erythropoiesis after PHZ treatment, on day 5 (C-D), day 7 (E-F), day 9 (G-H), and day 14 (I-J). Scale is shown.

Discussion

This analysis of Dhh mutant mice showed that Dhh is a negative regulator of differentiation of erythroid progenitors, as multiple stages of their development. Differentiation from CMP to GMP was decreased in Dhh$^{-/-}$ BM, indicating that Dhh is required for granulocyte/macrophage lineage differentiation. Interestingly, in the Dhh$^{-/-}$ BM, although the proportion of GMP was decreased, there was an increase in both CMP and MEP populations, so that in the absence of Dhh, erythroid differentiation was favored. Analysis of subsequent BFU-E and erythroblast populations revealed that Dhh negatively regulated multiple stages of erythroid lineage differentiation. In addition, after recovery from nonlethal radiation, and on induction of stress-induced anemia by PHZ treatment, differentiation in both spleen and BM was accelerated. We did not find evidence that absence of Dhh increased proliferation in the erythroblast populations, so the increased number of erythroblasts in the spleen and BM seemed to be the result of both the increase in early progenitors (CMP and MEP) and increased rate of differentiation.

The reduction in differentiation from CMP to GMP, mature granulocyte numbers, proportion of macrophages after irradiation, and of neutrophils after PHZ treatment, in the Dhh$^{-/-}$ BM is consistent with a recent study showing that Gli1 plays a role in myeloid differentiation.[5] In that study, the influence of Gli1 deficiency on erythroblast differentiation was not investigated.[5] It is, however, in contrast to recent reports that conditional deletion of Smo from hematopoietic lineage cells has no impact on any stage of hematopoiesis.[6,7,12] The reason for this difference is not clear, although it has been suggested that noncanonical Gli1-activation may be involved in the regulation of hematopoiesis.[5,12]

The impact of conditional deletion of Smo from hematopoietic cells has also been examined in stress-induced hematopoiesis in the spleen. Smo-deficient cells were found to be unable to respond to BMP4 and to recover normally after stress induction.[35] Although this study would seem to contradict reports that Smo deficiency has no impact on hematopoiesis,[6,7,12] it is possible that specific Smo-dependent mechanisms are important during the stress response in the spleen. In contrast, our data indicate that recovery and erythropoiesis in spleen and BM are accelerated in Dhh$^{-/-}$ mice. The reason for this discrepancy may lie in the fact that Smo is thought to be the essential nonredundant signal transduction component of the Hh signaling pathway, so Smo-deficient cells should be unable to transduce a Hh signal.[22] Dhh, however, is one of 3 Hh family members, and both Ihh and Shh are also expressed in the spleen.[35,45] Thus, although erythroblasts undergoing differentiation in the Dhh$^{-/-}$ spleen would have reduced Hh pathway activation, some Hh signal transduction was present (Figure 2), whereas Smo-deficient erythroblasts would be assumed to have none. Hh proteins can function as morphogens, signaling for distinct outcomes dependent on strength and duration of signal received.[21] Thus, it is possible that reduction in Hh signal (by Dhh deficiency) could produce the distinct outcome of accelerating stress-induced erythropoiesis in the spleen, compared with Smo deficiency, which resulted in reduced stress-induced erythropoiesis. Indeed, in the thymus, several experimental systems have shown that reduction of Hh signal accelerated pre-TCR induced differentiation, although some Hh signal transduction was still required for differentiation.[2,17,31]

Table 1. The ratio of red pulp/white pulp and percentage of red pulp in control and PHZ-treated WT and Dhh$^{-/-}$ spleen

	Red pulp/white pulp		Red pulp, %	
	WT	Dhh$^{-/-}$	WT	Dhh$^{-/-}$
Day 0	1.4	2.1	59	68
Day 5	5.2	4.8	84	83
Day 7	4.8	6.2	83	86
Day 9	5.0	4.9	83	83
Day 14	3.7	2.5	79	71

Red pulp and white pulp and entire surface area of longitudinal sections of paraffin-embedded spleen from WT and Dhh$^{-/-}$ mice, untreated (day 0), and at time points after PHZ treatment. Ratio of red pulp and white pulp and percentage of red pulp were quantified using ImageJ software.

In contrast to our finding that Dhh negatively regulates erythrocyte differentiation, Ihh has been shown to promote the earliest stages of hematopoiesis and vasculogenesis[13] and to support definitive erythropoiesis[10] in the mouse embryo. These opposing functions of Ihh and Dhh can be accounted for the different spatial and temporal expression patterns of the 2 genes, strength of signal transduced by each protein, and stage of differentiation on which they act, or by differences between embryonic and adult erythropoiesis. In our study, Dhh acted at multiple stages of erythrocyte differentiation from the LSK stage onwards, but we did not find an influence of Dhh deficiency on the LSK stem cells.

In conclusion, we have shown that Dhh signaling is a negative regulator of erythropoiesis, thus adding erythropoiesis to the very few functions currently ascribed to Dhh. This finding is of general importance to an understanding of erythropoiesis and may in the future have relevance to the treatment of human hematologic disease, including blood cancers and anemia.

Acknowledgments

The authors thank Ayad Eddaoudi (Institute of Child Health flow cytometry facility) for cell sorting, Bertrand Vernay for advice on Image analysis, and Great Ormond Street Hospital Histopathology for histology.

This work was supported by the Wellcome Trust, Medical Research Council, and Biotechnology and Biological Sciences Research Council. A.L.F. was supported by Great Ormond Street Hospital/University College London Institute of Child Health Biomedical Research Center, which received funding from the Department of Health's National Institute for Health Research Biomedical Research Centres funding scheme.

Authorship

Contribution: C.-i.L. and S.V.O. were major contributors of the data; C.-i.L. and T.C. wrote the manuscript; and all authors performed experiments.

Conflict-of-interest disclosure: The authors declare no competing financial interests.

Correspondence: Tessa Crompton, Immunobiology Unit, University College London Institute of Child Health, 30 Guilford St, London, WC1N 1EH, United Kingdom; e-mail: t.crompton@ucl.ac.uk.

References

1. Crompton T, Outram SV, Hager-Theodorides AL. Sonic hedgehog signalling in T-cell development and activation. *Nat Rev Immunol.* 2007;7(9):726-735.
2. Outram SV, Hager-Theodorides AL, Shah DK, et al. Indian hedgehog (Ihh) both promotes and restricts thymocyte differentiation. *Blood.* 2009; 113(10):2217-2228.
3. Zacharias WJ, Madison BB, Kretovich KE, et al. Hedgehog signaling controls homeostasis of adult intestinal smooth muscle. *Dev Biol.* 2011; 355(1):152-162.
4. Gritli-Linde A, Hallberg K, Harfe BD, et al. Abnormal hair development and apparent follicular transformation to mammary gland in the absence of hedgehog signaling. *Dev Cell.* 2007;12(1):99-112.
5. Merchant A, Joseph G, Wang Q, Brennan S, Matsui W. Gli1 regulates the proliferation and differentiation of HSCs and myeloid progenitors. *Blood.* 2010;115(12):2391-2396.
6. Hofmann I, Stover EH, Cullen DE, et al. Hedgehog signaling is dispensable for adult murine hematopoietic stem cell function and hematopoiesis. *Cell Stem Cell.* 2009;4(6):559-567.
7. Gao J, Graves S, Koch U, et al. Hedgehog signaling is dispensable for adult hematopoietic stem cell function. *Cell Stem Cell.* 2009;4(6):548-558.
8. Dierks C, Beigi R, Guo GR, et al. Expansion of Bcr-Abl-positive leukemic stem cells is dependent on Hedgehog pathway activation. *Cancer Cell.* 2008;14(3):238-249.
9. Zhao C, Chen A, Jamieson CH, et al. Hedgehog signalling is essential for maintenance of cancer stem cells in myeloid leukaemia. *Nature.* 2009; 458(7239):776-779.
10. Cridland SO, Keys JR, Papathanasiou P, Perkins AC. Indian hedgehog supports definitive erythropoiesis. *Blood Cells Mol Dis.* 2009;43(2): 149-155.
11. Siggins SL, Nguyen NY, McCormack MP, et al. The Hedgehog receptor Patched1 regulates myeloid and lymphoid progenitors by distinct cell-extrinsic mechanisms. *Blood.* 2009;114(5):995-1004.
12. Merchant AA, Matsui W. Smoothening the controversial role of hedgehog in hematopoiesis. *Cell Stem Cell.* 2009;4(6):470-471.
13. Dyer MA, Farrington SM, Mohn D, Munday JR, Baron MH. Indian hedgehog activates hematopoiesis and vasculogenesis and can respecify prospective neurectodermal cell fate in the mouse embryo. *Development.* 2001;128(10): 1717-1730.
14. Bitgood MJ, Shen L, McMahon AP. Sertoli cell signaling by Desert hedgehog regulates the male germline. *Curr Biol.* 1996;6(3):298-304.
15. St-Jacques B, Hammerschmidt M, McMahon AP. Indian hedgehog signaling regulates proliferation and differentiation of chondrocytes and is essential for bone formation. *Genes Dev.* 1999;13(16): 2072-2086.
16. Chiang C, Litingtung Y, Lee E, et al. Cyclopia and defective axial patterning in mice lacking Sonic hedgehog gene function. *Nature.* 1996; 383(6599):407-413.
17. Shah DK, Hager-Theodorides AL, Outram SV, Ross SE, Varas A, Crompton T. Reduced thymocyte development in sonic hedgehog knockout embryos. *J Immunol.* 2004;172(4):2296-2306.
18. Razzaque MS, Soegiarto DW, Chang D, Long F, Lanske B. Conditional deletion of Indian hedgehog from collagen type 2alpha1-expressing cells results in abnormal endochondral bone formation. *J Pathol.* 2005;207(4):453-461.
19. Zhang XM, Ramalho-Santos M, McMahon AP. Smoothened mutants reveal redundant roles for Shh and Ihh signaling including regulation of L/R symmetry by the mouse node. *Cell.* 2001;106(2): 781-792.
20. Parmantier E, Lynn B, Lawson D, et al. Schwann cell-derived Desert hedgehog controls the development of peripheral nerve sheaths. *Neuron.* 1999;23(4):713-724.
21. Ashe HL, Briscoe J. The interpretation of morphogen gradients. *Development.* 2006;133(3):385-394.
22. Ingham PW, Placzek M. Orchestrating ontogenesis: variations on a theme by sonic hedgehog. *Nat Rev Genet.* 2006;7(11):841-850.
23. Ingham PW, McMahon AP. Hedgehog signaling in animal development: paradigms and principles. *Genes Dev.* 2001;15(23):3059-3087.
24. Park HL, Bai C, Platt KA, et al. Mouse Gli1 mutants are viable but have defects in SHH signaling in combination with a Gli2 mutation. *Development.* 2000;127(8):1593-1605.
25. Gering M, Patient R. Hedgehog signaling is required for adult blood stem cell formation in zebrafish embryos. *Dev Cell.* 2005;8(3):389-400.
26. Detmer K, Thompson AJ, Garner RE, Walker AN, Gaffield W, Dannawi H. Hedgehog signaling and cell cycle control in differentiating erythroid progenitors. *Blood Cells Mol Dis.* 2005;34(1):60-70.
27. Detmer K, Walker AN, Jenkins TM, Steele TA, Dannawi H. Erythroid differentiation in vitro is blocked by cyclopamine, an inhibitor of hedgehog signaling. *Blood Cells Mol Dis.* 2000;26(4):360-372.
28. Bhardwaj G, Murdoch B, Wu D, et al. Sonic hedgehog induces the proliferation of primitive human hematopoietic cells via BMP regulation. *Nat Immunol.* 2001;2(2):172-180.
29. Trowbridge JJ, Scott MP, Bhatia M. Hedgehog modulates cell cycle regulators in stem cells to control hematopoietic regeneration. *Proc Natl Acad Sci U S A.* 2006;103(38):14134-14139.
30. Andaloussi AE, Graves S, Meng F, Mandal M, Mashayekhi M, Aifantis I. Hedgehog signaling controls thymocyte progenitor homeostasis and differentiation in the thymus. *Nat Immunol.* 2006; 7(4):418-426.
31. Outram SV, Varas A, Pepicelli CV, Crompton T. Hedgehog signaling regulates differentiation from double-negative to double-positive thymocyte. *Immunity.* 2000;13(2):187-197.
32. Rowbotham NJ, Hager-Theodorides AL, Furmanski AL, et al. Sonic hedgehog negatively regulates pre-TCR-induced differentiation by a Gli2-dependent mechanism. *Blood.* 2009; 113(21):5144-5156.
33. Hager-Theodorides AL, Dessens JT, Outram SV, Crompton T. The transcription factor Gli3 regulates differentiation of fetal $CD4^-$ $CD8^-$ double-negative thymocytes. *Blood.* 2005;106(4):1296-1304.
34. Drakopoulou E, Outram SV, Rowbotham NJ, et al. Non-redundant role for the transcription factor Gli1 at multiple stages of thymocyte development. *Cell Cycle.* 2010;9(20):4144-4152.
35. Perry JM, Harandi OF, Porayette P, Hegde S, Kannan AK, Paulson RF. Maintenance of the

BMP4-dependent stress erythropoiesis pathway in the murine spleen requires hedgehog signaling. *Blood.* 2009;113(4):911-918.

36. Perry C, Soreq H. Transcriptional regulation of erythropoiesis: fine tuning of combinatorial multidomain elements. *Eur J Biochem.* 2002;269(15):3607-3618.
37. Zhang J, Socolovsky M, Gross AW, Lodish HF. Role of Ras signaling in erythroid differentiation of mouse fetal liver cells: functional analysis by a flow cytometry-based novel culture system. *Blood.* 2003;102(12):3938-3946.
38. Migliaccio AR. Erythroblast enucleation. *Haematologica.* 2010;95(12):1985-1988.
39. Kerenyi MA, Orkin SH. Networking erythropoiesis. *J Exp Med.* 2010;207(12):2537-2541.
40. Cerdan C, Bhatia M. Novel roles for Notch, Wnt and Hedgehog in hematopoesis derived from human pluripotent stem cells. *Int J Dev Biol.* 2010;54(6):955-963.
41. Socolovsky M. Molecular insights into stress erythropoiesis. *Curr Opin Hematol.* 2007;14(3):215-224.
42. Hager-Theodorides AL, Rowbotham NJ, Outram SV, Dessens JT, Crompton T. beta-Selection: abundance of TCRbeta(−)/gammadelta(−) CD44(−)CD25(−) (DN4) cells in the foetal thymus. *Eur J Immunol.* 2007;37(2):487-500.
43. Rowbotham NJ, Hager-Theodorides AL, Cebecauer M, et al. Activation of the Hedgehog signaling pathway in T-lineage cells inhibits TCR repertoire selection in the thymus and peripheral T-cell activation. *Blood.* 2007;109(9):3757-3766.
44. Hegde GV, Peterson KJ, Emanuel K, et al. Hedgehog-induced survival of B-cell chronic lymphocytic leukemia cells in a stromal cell microenvironment: a potential new therapeutic target. *Mol Cancer Res.* 2008;6(12):1928-1936.
45. Sacedon R, Diez B, Nunez V, et al. Sonic hedgehog is produced by follicular dendritic cells and protects germinal center B cells from apoptosis. *J Immunol.* 2005;174(3):1456-1461.